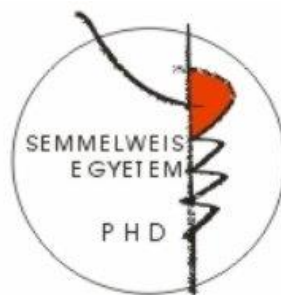


Mechanism of modulated electro-hyperthermia induced tumor destruction in C26 colorectal cancer models

Short thesis

Tamás Vancsik

Semmelweis University
Doctoral School of Pathological Sciences



Supervisor: Tibor Krenács, D.Sc.

Reviewers: István Kenessey, M.D., Ph.D.
Tamás Csonka, M.D., Ph.D.

Head of examining board: András Kiss, M.D., D.Sc.
Members of examining board: Tibor Glasz, M.D., Ph.D.
Lajos László, Ph.D.

Budapest
2019

1. Introduction

Modulated electro-hyperthermia treatment (mEHT, also called “oncothermia”) is a non-invasive complementary to chemo- and radio-therapy using electromagnetic field generated by amplitude modulated 13.56 MHz radiofrequency. The electromagnetic field, which can instantly penetrate into cancer lumps, induces heat shock response and cell stress at controlled 42°C, besides interfering with cell membrane lipid rafts gathering receptor molecules. Tumor selectivity of mEHT is linked to elevated glucose uptake (which has already been utilized in FDG-PET CT), glycolysis (also known as the Warburg effect) and the concomitant ion concentration and conductivity of tumors compared to adjacent normal tissues.

Loco-regional mEHT treatment has been exploited in combinations with chemo- and radio-therapy for successfully treating e.g. human gliomas, soft tissue sarcomas as well as cervical, colorectal and breast adenocarcinomas. Complementary mEHT treatment is financed by the national health insurances e.g. in Germany, Switzerland, Italy, Canada, South-Korea and Japan. However, the mechanism of action of tumor damage induced by mEHT and its molecular background have been insufficiently revealed. Therefore, we set up *in vitro* and *in vivo* tumor models for the better understanding.

We choosed C26 an aggressive mouse colorectal adenocarcinoma cell line in our mEHT treatment models. Colorectal cancer is one of the most common fatal malignancies worldwide, affecting more than 1.2 million new patients every year. At least 50% of the cases relapse after surgical removal of the tumor without distant metastasis, but 20% of colorectal cancers have distant metastasis at the time of diagnosis. Though the 5-year survival of localized cancer is over 90%, it is sharply reduced to <12% in patients with distant tumor spread.

In the studies of this PhD thesis we tested the molecular background of cell stress, apoptosis and damage associated molecular pattern (DAMP) related effects of mEHT treatment using C26 cell line. In an *in vitro* model we combined mEHT treatment with doxorubicin (Dox), which is an anthracycline anti-tumor antibiotic, frequently used in first-line chemotherapy. It can destruct cancer cells both by preventing DNA repair in proliferating cells and by generating reactive oxygen species (ROS). However, its use carries the risk of cardiotoxicity. The aim of this combination was to boost the anti-tumor effect of Dox which would allow to use it at lower concentrations with less side effects but similar efficiency.

Also, mEHT pre-treatment has recently been described to augment tumor antigen primed dendritic cell immunotherapy through supporting T-cell, macrophage and eosinophil leukocyte invasion. Therefore, in an allograft model of C26 cancer cells we also tested the

potential immune promoting effect of mEHT, which may result in tumor destruction at distant tumor nodules.

Better understanding of the mechanism of action of mEHT in malignant tumors, can support designing it more efficient treatment combinations with chemo-, radio- and even with targeted oncotherapies.

2. Aim of study

My work aimed at investigating the molecular background and the dynamics of mEHT induced cancer damage in C26 colorectal adenocarcinoma cell line models by focusing on:

- The cell stress and death induced by mEHT treatment *in vitro*.
- The tumor damage mechanisms induced by doxorubicin alone and in combination with mEHT treatment *in vitro*.
- The cell stress and programmed cell death pathways induced by mEHT treatment in C26 tumor allografts in immunocompetent BALB/c mice.
- The compatibility of the *in vitro* and *in vivo* model systems.
- The spatio-temporal expression and release of DAMP signaling molecules in the locoregionally mEHT treated tumors.
- The occurrence of immune cells in and around the treated tumors in relation to tumor damage, thus the potential systemic anti-tumor effect of mEHT treatment.

3. Materials and methods

Cell culturing: C26 murine colorectal adenocarcinoma cell line was used for both *in vitro* and *in vivo* experimental models.

***In vitro* doxorubicin and modulated electro-hyperthermia treatments:** Subconfluent coverslip cultures were mEHT treated (13.56 MHz amplitude modulated radiofrequency) for 2x30 min at 42°C between two plan-parallel electric condenser plates by using the Lab-EHY 100 device with a 120 min break in between treatments. After the second intervention cultures were put into fresh culture medium or in combined treatment the medium contained 1 µM doxorubicin (mEHT+Dox). mEHT-untreated cultures got fresh medium (control) or 1 µM doxorubicin (Dox).

qRT-PCR: The expression of mEHT-induced apoptosis and cell cycle control related genes were tested. mRNA was extracted 1, 3, 9 and 24 h after mEHT treatment. Quantitative PCR testing of RpLp0 (housekeeping gene), PUMA, BAX, BAK1, XIAP, BCL-2, BCL-XL,

and P21 target gene expression. The fold change of the genes of interest relative to RpLp0 was defined as $2^{-\Delta\Delta CT}$ method.

Viability and doxorubicin uptake measurements: Samples from the cell culture medium were collected for measuring Dox uptake using 530/590 or 570/590 nm (excitation/emission) filter pairs of the fluorometer. 24 and 48 hours post-treatment resazurin viability assay was performed.

Measurement of apoptosis-necrosis ratio: 24 h after treatment, the supernatant and the cells were collected. For identifying apoptotic and necrotic fractions cell cultures were stained with FITC-Annexin V (green) and propidium-iodide (red) then analyzed by flow cytometry.

Cell cycle and subG₁ fraction analysis: Propidium-iodide and flow cytometry was also used for measuring the changes in the cell cycle of cell populations and confirming the termination of apoptosis by counting cells in subG₁-phase.

Polarized membrane staining: Mitochondrial membrane integrity was tested using 3,3'-dihexyloxycarbocyanine iodide staining (DiOC6) measured by flow cytometry.

Immunostaining for flow cytometry: 24 h after mEHT treatment supernatants and cells were collected then counted in a Bürker-chamber. Paraformaldehyde-fixed and permeabilized cell cultures were immunolabelled by using Alexa Fluor® 488 conjugated rabbit monoclonal phospho-Akt^{Ser473} and cleaved caspase-8(Asp387) and phospho-p53^{Ser15} antibodies. For detecting unlabeled rabbit antibodies an Alexa Fluor 488 conjugated IgG was used. On negative controls a primary antibody was not used.

Immunocytochemistry, hematoxylin-eosin staining and image analysis: Fixed and permeabilized cell cultures were hematoxylin-eosin and immuno-stained for calreticulin, cleaved caspase-3, Hsp70, phospho-H2AX^{Ser139} and p53. Detection was done with immunofluorescent labelling and also by chromogen reaction. Coverslip cultures were mounted onto glass slides then digitalized and evaluated with Quant center software modules.

Clonogenic assay: 24 h after treatment, 500 cells/well were cultured for 10 days, then fixed and stained with crystal violet for counting the tumor-progenitor colonies.

In vivo tumor model: C26 murine colorectal adenocarcinoma cell line was subcutaneously injected with 10⁶/0.1 ml density into both femoral region of immunocompetent 6 weeks old BALB/c mice (females). Thereafter animals were kept for 14 days until the diameter of symmetrical tumor implants reached ~1.5 cm diameter.

In vivo modulated electro-hyperthermia and Marsdenia tenacissima extract (MTE) treatment: Right leg tumors were treated with a single shot of mEHT (mEHT_{right}) of the symmetrical C26 allografts using plan-parallel electric condenser plates embracing the tumors. The left-leg tumors served both for untreated internal controls (mEHT_{left}) and for

monitoring the systemic effect. Intratumoral temperature of mEHT_{right} was measured with optical sensors and kept at ~42°C (+/- 0.5°C). The subcutaneous temperature under the electrode was kept at ~40 °C and the rectal temperature at ~37°C. The chlorogenic acid rich *Marsdenia tenacissima* plant extracts (MTEs), have been shown to increase chemo-sensitivity of tumors and promote T-cell activation. Mice were injected with 7.5 ml/kg extract intraperitoneally (i.p.). In the combined treatment group, MTE administration was followed 30 min later by mEHT treatment of the right-leg tumors (mEHT+MTE_{right}). In sham treated control animals the experimental conditions were the same as in mEHT groups except that the electric circuit was turned off. Tumor samples were collected 12, 24, 48 and 72 h after treatment following the termination of mice. Excised tumors were fixed in formalin, dehydrated and embedded into paraffin wax.

Immunohistochemistry and TUNEL assay: Both whole cross sections and tissue microarrays (TMA) were used for immunohistochemistry for the following target proteins: AIF, Bax, calreticulin, CD3, cleaved caspase-3, cleaved caspase-8, cytochrome-c, FoxP3, HMGB1, Hsp70, S100. Slides were digitalized and evaluated with Quant center software modules.

Measuring the tumor destruction: Sections from whole tumor blocks were used for hematoxylin-eosin staining. Based on image color and intensity segmentation, the whole tumor area (W) was correlated with the damaged (paler) tumor tissue (D) for calculating the tumor destruction ratio (TDR=W/D) on digital slides.

Statistics: In case of the *in vitro* results statistical analysis for parametric variables was done with the independent two-sample t-test using Microsoft Excel Analysis ToolPak Add-In software. For non-parametric variables the Kuskal-Wallis test with the Mann-Whitney U-test for pairwise comparisons, were applied. For the *in vivo* experiments non-parametric test was used, followed by Dunn's post hoc test with Bonferroni correction.

4. Results

4.1. *In vitro* mEHT monotherapy

In subconfluent C26 colorectal adenocarcinoma cultures 24 h after 2x30 min mEHT monotherapy (at 42°C) significant upregulation and relocalization of calreticulin from the endoplasmic reticulum to the cytoplasm and cell membranes was observed in treated cultures besides the blebbing of calreticulin positive cell membranes. Also, increased the proportion of tumor cells showing elevated Hsp70 levels. Furthermore, the median intensity of the cleaved caspase-8 positive cell fraction was also increased, while the polarized membrane-staining of DiOC6 indicating intact mitochondrial membranes, was significantly reduced after mEHT.

mEHT monotherapy induced a major mRNA fold-decrease of the anti-apoptotic BCL-2, BCL-XL and XIAP transcripts both after 1 h and 3 h post-treatment, while the pro-apoptotic BAX showed a moderate but prolonged increase after 1 h and 9 h. The pro-apoptotic PUMA and the cyclin dependent kinase inhibitor P21 transcript levels also revealed significant increase at 1 h, 3 h and 9 h post-treatment. These changes were accompanied by the elevation of the cleaved/activated caspase-3 protein positive tumor cell density in the treated cultures.

In clonogenic assay colony formation from tumor progenitor/stem cell clones was significantly reduced after mEHT monotherapy.

4.2. *In vitro* doxorubicin treatment combined with mEHT

After 24 h mEHT reduced tumor cell viability to $87.35\pm 6.36\%$, Dox treatment to 56.92 ± 2.62 while their combination resulted in only $25.00\pm 3.31\%$ surviving tumor cells at 24 h. 48 h after mEHT treatment cell viability was further reduced to $78.82\pm 5.84\%$, $29.06\pm 1.89\%$ and $13.17\pm 2.48\%$, respectively. The number of surviving tumor cells also showed strong correlation with the resazurin assay particularly after combined treatment.

Combination of mEHT with Dox concentration in culture supernatants were reduced to 0.70 ± 0.07 fold of those of Dox monotherapy suggesting the promotion of drug uptake.

Dox at 1 μM concentration, both alone and in combination with mEHT, completely killed tumor progenitor cell clones.

Survival related Akt kinase activation was measured through the phospho-Akt^{Ser473} positive cell fractions, which showed a strong tendency of reduction after both mEHT and mEHT+Dox treatments compared to control. At the same time, the activated tumor-suppressor phospho-p53^{Ser15} protein positive cell populations were significantly increased after mEHT, Dox and after combined treatments. With immunocytochemistry, elevated number of tumor cells showing nuclear translocation of the p53 protein was detected in the treated cultures indicating the stabilization and activation p53 protein.

mEHT monotherapy induced a significant increase of the apoptotic tumor cell fractions ($14.53\pm 2.99\%$) compared to the untreated cultures ($1.94\pm 0.36\%$). At the same time, apoptosis was not significant ($2.31\pm 0.73\%$) after Dox treatment. This finding was further supported by the combined mEHT+Dox treatment resulting in only similar proportions of apoptotic cell populations ($16.67\pm 3.69\%$) to mEHT monotherapy. Necrotic cell populations were detected also in the control cultures ($6.24\pm 2.64\%$), which are increased more after Dox monotherapy ($11.18\pm 1.50\%$) than after mEHT ($9.84\pm 1.25\%$) and these were added together after combined treatment ($20.63\pm 11.36\%$) (Figure 16A).

The proportion of cells with apoptosis-related fragmented DNA in subG₁-phase was grown significantly from 1.92±0.16% to 16.47±1.64% after mEHT, to 3.13±0.94 after Dox and to 17.27±2.99% after combined mEHT+Dox treatments. DNA double strand-breaks indicated by the increased intensity and granularity of the H2AX γ immunoreaction in tumor cell nuclei, was also detected at high levels both after mEHT monotherapy and after combined mEHT+Dox therapy compared to controls.

G₁-phase cell populations in the cell cycle were significantly reduced both after mEHT, Dox and mEHT+Dox treatments. S-phase cell populations showed decrease only after Dox monotherapy, while G₂-phase cell fractions were increased after both monotherapies, but more in case of Dox. mEHT+Dox treatment caused an intermediate increase compared to the monotherapies.

4.3. *In vivo* local mEHT and systemic MTE treatment

TDR was significantly higher in mEHT treated (mEHT_{right}) than untreated sides (mEHT_{left}) or sham control tumors between 24-72 h post-treatment. Combination therapy (mEHT+MTE) led to tumor damage not only in the treated right tumors (mEHT+MTE_{right}) but also in the untreated left tumors (mEHT+MTE_{left}) within the same time-frame. The effect of MTE administration alone was negligible.

Nuclear chromatin condensation and widespread apoptotic bodies indicated mEHT induced programmed cell death response from 24 h post-treatment. It was confirmed by the elevated number of cell nuclei with fragmented DNA indicated by TUNEL assay. Post hoc test revealed significant elevation in TUNEL positivity: in mEHT_{right} vs. sham controls; in the mEHT+MTE_{right} or mEHT+MTE_{left} vs. sham controls and mEHT_{left}.

mEHT treatment induced the significant mitochondrial translocation of Bax protein and the cytoplasmic release of cytochrome-c between 12 and 24 h in the treated (mEHT_{right}) tumors either after single or combined mEHT treatment. Cytochrome-c became significantly delocalized also in the mEHT untreated (left-leg) tumors of the combined mEHT+MTE group between 48-72 h. There was no statistical difference in nuclear AIF levels between the treated and untreated tumors. Major elevation of cleaved/activated caspase-3 positive cell numbers was seen from 12 h post-treatment compared to sham controls. Overlapping cleaved caspase-8, -caspase-3 and TUNEL positive cell fractions were significantly elevated in the apoptotic tumor regions including the intact-damaged marginal zone, particularly at advanced stages, 48-72 h post-mEHT treatment. These findings are consistent with the activation of caspase-dependent extrinsic and intrinsic apoptotic pathways. After treatment, the nuclear Ki67

protein expression disappeared completely from tumor cells which showed minor morphological signs of apoptosis.

4.4. *In vivo* mEHT and MTE treatment induced stress and damage associated molecular pattern signaling

Massive cytoplasmic to cell-membrane relocation of calreticulin was observed from 12 h post-treatment, which was significantly higher in mEHT_{right} than in mEHT_{left} and sham control tumors; in mEHT+MTE_{right} or mEHT+MTE_{left} than in mEHT_{left} and sham control tumors. This was followed by the significant cell-membrane accumulation of Hsp70 protein in the mEHT-treated groups peaking at 48 h post-treatment. Pairwise significance was seen in mEHT_{right} vs. mEHT_{left} and sham control tumors; and in mEHT+MTE_{right} or mEHT+MTE_{left} vs. mEHT_{left} and sham control tumors. Significant nuclear to cytoplasmic release or complete loss in the damaged areas of HMGB1 protein was also seen at 48 h post-mEHT treatment. Post hoc test confirmed significant disappearance of HMGB1 in mEHT_{right} vs. sham controls; and in mEHT+MTE_{left} vs. mEHT_{left} tumors.

4.5. *In vivo* mEHT and MTE treatment induced immune response

DAMP signal sequence was accompanied by the massive tumor infiltration by S100 positive APC from 48 h post-treatment, which was significantly higher in mEHT_{right} compared to mEHT_{left} and sham tumors; and in mEHT+MTE_{right} compared to sham tumors. Also, significant numbers of CD3 positive T-cells infiltrated the treated tumors with a peak at 72 h post-mEHT treatment. Pairwise testing confirmed significantly more T-cells in mEHT_{right} vs. mEHT_{left} tumors; in mEHT+MTE_{right} vs. sham_{left} and sham_{right} tumors. APC and T-cell invasion also showed a nearly significant trend between mEHT+MTE_{left} and sham control tumors. A dense ring of T-cell invasion was seen in the margin between the damaged and the “intact”-looking tumor regions, furthermore, the latter was also infiltrated heavily. FoxP3 positive T-cells were rare and their number did not differ between treated and untreated tumors.

5. Conclusion

mEHT treatment induced significant tumor damage *in vitro* and *in vivo*. This was preceded by the early downregulation of the anti-apoptotic XIAP, BCL-2 and BCL-XL and elevation of pro-apoptotic BAX and PUMA transcripts *in vitro*. These were followed by the upregulation of activated caspase-8 and -3 proteins at the same time with the reduction of DiOC6 polarized membrane-dye intensity, which were consistent with the activation of both the extrinsic and intrinsic apoptosis. mEHT treatment induced significant DNA double strand-breaks indicated by nuclear deposition of H2AX γ besides the upregulation of phospho-p53^{Ser15} and p21^{waf1}. These were in line with the blockade of cell cycle (senescence) and the reduction of tumor stem cell colonies. Also *in vitro*, mEHT induced apoptosis, while doxorubicin (Dox) treatment led to necrosis. Furthermore, mEHT promoted the Dox uptake and the combined treatment additively reduced tumor cell viability and augmented cell death near to synergy. The upregulation and release of damage associated molecular pattern (DAMP) signals including Hsp70, calreticulin and HMGB1 proteins were relevant for inducing immunogenic cell death (ICD) response *in vivo*. Indeed, a single shot of mEHT led to progressive tumor damage and accumulation of CD3+ T-cells (with scant FoxP3+ regulatory T-cells) and S100+ antigen presenting dendritic cells. Immune mediated tumor damage was also observed in the untreated contralateral tumors when mEHT was combined with a chlorogenic acid rich T-cell promoting MTE agent, indicating a systemic anti-tumor effect of mEHT treatment.

In conclusion, both the *in vitro* and *in vivo* showed that mEHT treatment alone can induce DNA double-strand breaks and irreversible cell stress leading to both caspase-dependent apoptosis and the release of stress associated DAMP proteins in colorectal cancer models. *In vitro* data revealed that p21^{waf1} mediated growth arrest and apoptosis were likely be driven by the upregulated nuclear p53 protein. Elevated phospho-p53^{Ser15} might contribute to p53 escape from mdm2 control. In combinations, mEHT promoted the uptake and significantly potentiated the cytotoxic effect doxorubicin. *In vivo*, a single shot of mEHT induced progressive apoptosis driven tumor cell death in parallel with the increasing infiltration of immune cells within and around the tumors. Accumulating antigen presenting dendritic cells and T-cells are likely to contribute to the ongoing secondary tumor destruction by an immunogenic cell death (ICD) mechanism both locally and through a systemic effect at distant tumor sites. Clarifying the mechanism of action of the tumor damaging effect of mEHT treatment can support its more rational designing of treatment combinations in human oncotherapy.

Publications relevant to the dissertation

Vancsik T, Kovago C, Kiss E, Papp E, Forika G, Benyo Z, Meggyeshazi N, Krenacs T. Modulated electro-hyperthermia induced loco-regional and systemic tumor destruction in colorectal cancer allografts. *Journal of Cancer*. 2018;9(1):41-53. IF: 3.182

Vancsik T, Forika G, Balogh A, Kiss E, Krenacs T. Modulated electro-hyperthermia (mEHT) induced p53 driven apoptosis and cell cycle arrest additively support doxorubicin chemotherapy of colorectal cancer *in vitro*. *Cancer Medicine*. 2019;00:1–12. IF: 3.357

Other publications

Rajnai H, Teleki I, Kiszner G, Meggyeshazi N, Balla P, Vancsik T, Muzes Gy, Csomor J, Matolcsy A, Krenacs T. Connexin 43 communication channels in follicular dendritic cell development and in follicular lymphomas. *Journal of immunology research*. 2015;2015:528098. IF: 2.812

Acknowledgements

I am grateful for Dr. Tibor Krenács for providing the opportunity to work in his laboratory and for supervising my work all the time.

I am thankful to Prof. András Matolcsy to let me work in his institution and to Prof. Ilona Kovalszky that I could study in the Pathology Doctoral School.

I am grateful for all the members of the laboratory, especially for Edit Parsch† and Éva Mátrainé Balogh for their excellent technical support in the laboratory work, to András Sztodola for his help in the animal experiments, and to Marica Csorba Gézáné† and Titanilla Dankó for their support in cell culturing.

I am also thankful for all of my former and recent colleagues: Éva Kiss, Gertrúd Fórika, Nóra Meggyesházi, Péter Balla, Lilla Füleki for their help and friendly atmosphere; and to Dr. Csaba Kővágó, who guided me at the first steps in the animal experiments and to Edina Papp for helping in data analysis.

I am thankful to Dr. Gábor Barna and Orsi Szabó for their patient teaching and help in flow cytometry.

Many thanks to Prof. Zoltán Benyó for his motivating attitude and for letting me work with his colleagues in the Institute of Clinical Experimental Research, in particular to Andrea Balogh for her advices and guidance in the *in vitro* studies.

I am also grateful to all members of the 1st Department of Pathology and Experimental Cancers Research who helped me in any aspect of my studies.

Furthermore, I am thankful to Prof. András Szász for supporting me with professional advice.

Finally, but not least, I am truly grateful to my beloved family and friends who give me the stable background and motivation throughout my work.